

## On the removal of the non-uniqueness in the solution of elastostatic problems by symmetric Galerkin BEM

R. Vodička<sup>1,‡</sup>, V. Mantič<sup>2,\*</sup>,† and F. París<sup>2,§</sup>

<sup>1</sup>*Department of Mathematics, Faculty of Civil Engineering, Technical University of Košice, Vysokoškolská 4, 042 02 Košice, Slovakia*

<sup>2</sup>*Group of Elasticity and Strength of Materials, School of Engineering, University of Seville, Camino de los Descubrimientos s/n, 41092 Seville, Spain*

### SUMMARY

A study of the removal of the non-uniqueness in the solution of elastostatic problems by means of the *symmetric Galerkin boundary element method* is presented. The paper focuses on elastic problems defined on domains with cavities, where cavity boundaries are subjected to traction boundary conditions. A simple method consisting in a direct application of support conditions and several methods based on the Fredholm theory of linear operators are introduced, implemented and analysed. Numerical examples demonstrate the performance of the proposed methods and accuracy of their results, a comparative evaluation of the methods developed being finally presented. Copyright © 2005 John Wiley & Sons, Ltd.

**KEY WORDS:** symmetric Galerkin boundary element method (SGBEM); boundary integral equations (BIE); rigid body motion; solution uniqueness; Fredholm theory; domain with cavities; linear elasticity

### 1. INTRODUCTION

The symmetric Galerkin BEM (SGBEM) [1, 2] is an advanced and promising variant of the direct BEM technique. It provides, unlike the classical collocational BEM [3, 4], symmetric matrices and excellent convergence properties in energy norms. SGBEM is also considered to

---

\*Correspondence to: V. Mantič, Group of Elasticity and Strength of Materials, School of Engineering, University of Seville, Camino de los Descubrimientos s/n, 41092 Seville, Spain.

†E-mail: mantic@esi.us.es

‡E-mail: Roman.Vodicka@tuke.sk

§E-mail: paris@esi.us.es

Contract/grant sponsor: Scientific Grant Agency of the Slovak Republic; contract/grant numbers: 1/8033/01, 1/1089/04

Contract/grant sponsor: Spanish Ministry of Education and Culture; contract/grant number: MAT2003-03315

be useful, in particular, for crack analysis and for coupling with finite element method (FEM). For a comparison of SGBEM and collocational BEM see, e.g. References [5, 6].

The present work has been motivated by the fact, perhaps at first sight surprising, that there are elastic boundary value problems (BVPs) whose SGBEM solutions are non-unique (in other words the corresponding linear operators are non-invertible) whereas the BVPs are uniquely solvable.

A domain whose boundary includes one or several non-intersecting closed surfaces in three-dimensional problems (or closed curves in plane problems) different from the outer boundary will be referred to hereinafter as *domain with cavities*. Note that there exists also a different concept of holes in a 3-D body, see Reference [7] for details and other references. It is also important to realize that in the 2-D case both concepts, cavities and holes, are coincident.

Then, an SGBEM solution is non-unique for any BVP defined on a domain with cavities when tractions are prescribed on some of its cavities. A particular example of such a BVP is a solid with a traction-free cavity, independently of the boundary conditions prescribed along the outer boundary. This non-uniqueness appears due to the application of the hypersingular boundary integral equation (HBIE) in the formulation of the SGBEM for such a cavity. It will be shown that displacements defined by a rigid body motion (RBM) of the cavity boundary can be freely added to a solution of the HBIE, the result of this operation still being a solution of this HBIE. Note that this statement holds even in the case where the outer boundary surface of the body is clamped.

The above-explained problem has apparently not captured significantly the attention of the direct-BEM community, in proportion to the importance of the problem. There is only a small number of previous publications where this difficulty has been mentioned, e.g. Reference [6], or some approaches to solve this problem have been proposed, e.g. Reference [8] for external problems (with an unbounded domain). Implementations in an SGBEM code of some methods dealing with this non-uniqueness have only recently appeared [9, 10].

It should be pointed out that a similar phenomenon of a non-unique solution represents a well-known difficulty in the so-called indirect BEM, appearing when the double layer potential is used to represent a solution. A method for the elimination of this non-uniqueness is the completed double layer boundary element method, which was introduced in the field of Stokes flow problems in References [11–13] and later also utilized in elastic problems in References [14, 15]. The idea of this method is quite close to one of the methods studied in the present paper and is based on the completion of the range and simultaneous modification of the kernel of the double-layer operator to obtain an invertible full-range operator.

Several methods for the removal of the non-uniqueness in the solution of elastic BVPs by SGBEM caused by the presence of either an RBM of the whole body in the solution of a traction BVP or an RBM of a cavity boundary with prescribed traction boundary conditions are developed and studied simultaneously in the present work.

Although the aforementioned papers [9, 10] deal with the same topic, it should be stressed that a slight perturbation of the symmetry of the resulting linear system arises when applying the methods introduced therein. Thus, these methods do not yield a purely symmetric Galerkin BEM.

Another, rather simple, approach of Reference [10] introduces auxiliary interior boundaries which split the domain into several subdomains in such a way that the resulting subdomains do not contain cavities. In any case, this approach introduces more variables in the discretized linear system and also raises a question about a suitable choice and an automatic generation of the auxiliary interior boundaries.

One of the advantages of the methods introduced in the present work in comparison with those developed in References [9, 10] is that they do not need either symmetry perturbation or auxiliary interior boundaries. The advantage of keeping the symmetry of the resulting linear system will, in addition to allowing a simple and standard programming in the framework of SGBEM, significantly decrease the computational resources required, in particular with reference to the storage of the linear system and the number of arithmetic operations in its solution.

The first method studied in the present work is related to a common method used in *matrix structural analysis*. It removes all the RBMs allowed by the problem configuration by imposing a required number of point supports (zero nodal values of displacements), which hinder these RBMs without modification of the solution in stresses, directly in the resulting linear system. Note that this simple method may cause, in classical collocation BEM, significant errors [16]. Such errors do not appear in the theoretically well-established methods (using the Fredholm theory of linear operators) presented and implemented in a classical collocation BEM code in Reference [16], see also Reference [17]. The crucial fact that this kind of error does not appear in SGBEM, when the discretized external loads are in equilibrium, even if the above-mentioned direct imposition of point supports (zero displacement values) is applied, was discussed in Reference [16] and numerically studied in Reference [18].

The Fredholm theory of linear operators and its application to operators of BIEs analysed theoretically and numerically in References [12, 13, 16, 18–20] is the base of the other non-uniqueness removal methods developed in the present work. In general terms, the non-uniqueness removal may be performed in two ways, either by augmenting the original non-invertible linear operator [8, 12, 13, 16, 18–21], or by adding an operator with a degenerate kernel to the original one [11–13, 15–18, 22].

In the present work a comparative study of the methods introduced here is presented. Relations between them and also some features of their implementation in an SGBEM code are discussed. All these methods have been implemented in a 2-D SGBEM code for isotropic linear elasticity. The numerical study presented has been performed with the aim of establishing some recommendations for practical SGBEM computations.

The authors would like to state that the present paper can be considered as a free continuation of works [16] and [18] in the sense that the methods for removal of RBMs in the solution of traction BVPs on domains without cavities successfully applied, respectively, in the classical collocation BEM and SGBEM therein are extended here to SGBEM for domains with cavities.

## 2. BIEs OF SGBEM FOR DOMAINS WITH CAVITIES AND THEIR NON-UNIQUE SOLUTION

### 2.1. Formulation of BIEs in elasticity

Let us consider an elastic body defined by a domain with cavities  $\Omega \subset \mathbb{R}^d$  ( $d=2, 3$ ) with a bounded Lipschitz piecewise smooth boundary  $\partial\Omega=\Gamma$  (domain  $\Omega$  is locally on one side of  $\Gamma$ ). Let  $\Gamma_S \subset \Gamma$  denote the smooth part of  $\Gamma$ , i.e. excluding corners, edges, points of curvature jumps, etc. For the sake of simplicity of explanation, the case of a domain with only one cavity will be considered in the main theoretical part of the present work, whereas a generalization

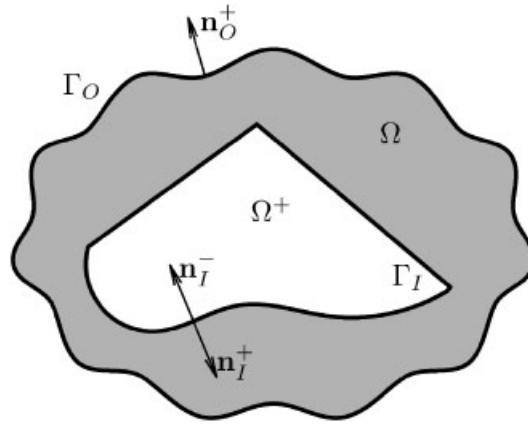


Figure 1. Description of a one-cavity domain.

to domains with more cavities is discussed in Appendix A. Figure 1 shows an example of a bounded one-cavity domain.

Let us denote  $\Omega^+$ , the domain that forms the cavity in  $\Omega$  and  $\Gamma_I = \partial\Omega^+$  its boundary. This means that when domain  $\Omega^+$  together with its boundary  $\Gamma_I$  is added to  $\Omega$ , a domain without cavities  $\Omega_O$  with the boundary  $\Gamma_O$  is obtained. It should be noted that  $\Omega$  can be unbounded. In such a case  $\Omega_O$  is equal to  $\mathbb{R}^d$  and  $\Gamma_O = \emptyset$ . Let us denote two normal vectors on  $\Gamma_I$  as  $\mathbf{n}_I^\pm$ , defined by the unit normal vectors which are outward (+) or inward (-) with respect to the domain  $\Omega^+$ . Finally, let us denote the outward unit normal vector at  $\Gamma_O$  by the symbol  $\mathbf{n}_O^+$ .

Let the traction operator  $\mathcal{F}$  give the traction vector  $\mathbf{t}(x)$  associated to a unit normal vector  $\mathbf{n}$  when applied to displacements  $\mathbf{u}(x)$  as follows:  $\mathbf{t}(x) = \mathcal{F}(\mathbf{n}, \partial_x)\mathbf{u}(x)$ . Somigliana displacement identity [3, 4, 23], considered here for the sake of brevity without body forces, can be expressed in the following form:

$$\chi_\Omega(x)u_k(x) = \int_\Gamma U_{kl}(x, y)t_l(y) d\Gamma(y) - \int_\Gamma T_{kl}(x, y)u_l(y) d\Gamma(y), \quad x \in \mathbb{R}^d \setminus \Gamma, \quad k, l = 1, \dots, d \tag{1}$$

where  $\chi_\Omega$  is the characteristic function of the domain  $\Omega$  ( $\chi_\Omega(x) = 1$  if  $x \in \Omega$  and  $\chi_\Omega(x) = 0$  if  $x \notin \Omega \cup \Gamma$ ),  $U_{kl}$  is the fundamental solution in displacements of Navier equation and  $T_{kl}$  represents the fundamental tractions, obtained from the fundamental solution via the traction operator as follows:  $\mathbf{T}(x, y) = (\mathcal{F}(\mathbf{n}(y), \partial_y)\mathbf{U}(x, y)\mathbf{t})^T$ ,  $\mathbf{n}(y)$  denoting the outward normal unit vector to  $\Gamma$  at  $y$  and  $T$  denoting the transpose matrix. Note that (1) is also valid for an exterior BVP defined on an unbounded region with a bounded boundary [3, 23] if the solution fulfils the well-known regularity condition at infinity:

$$u_k(x) = U_{kl}(x, 0)b_l + O(\|x\|^{1-d}), \quad \|x\| \rightarrow \infty, \quad b_l = \int_\Gamma t_l(y) d\Gamma(y) \tag{2}$$

Somigliana traction identity [3, 4] is obtained applying the traction operator to (1) as follows:

$$\chi_{\Omega}(x)t_k(x) = \int_{\Gamma} T_{kl}^*(x, y)t_l(y) \, d\Gamma(y) - \int_{\Gamma} S_{kl}(x, y)u_l(y) \, d\Gamma(y), \quad x \in \mathbb{R}^d \setminus \Gamma, \quad k, l = 1, \dots, d \tag{3}$$

where  $\mathbf{T}^*(x, y) = \mathcal{F}(\mathbf{n}(x), \partial_x)\mathbf{U}(x, y)$ ,  $\mathbf{S}(x, y) = \mathcal{F}(\mathbf{n}(x), \partial_x)\mathbf{T}(x, y)$  and  $\mathbf{n}(x)$  is a normal to an auxiliary curve or surface, depending on the dimension  $d$ , passing through the point  $x$  at which the traction is to be evaluated.

With reference to the above-defined integral kernels, let us recall the following reciprocity relations [1]:  $\mathbf{U}(x, y) = \mathbf{U}^T(y, x)$ ,  $\mathbf{T}^*(x, y) = \mathbf{T}^T(y, x)$  and  $\mathbf{S}(x, y) = \mathbf{S}^T(y, x)$ . Additionally, the fundamental solution is symmetric, i.e.  $\mathbf{U}(x, y) = \mathbf{U}^T(x, y)$ , and, according to Reference [24], the hypersingular integral kernel  $\mathbf{S}$  is also symmetric in 2-D, i.e.  $\mathbf{S}(x, y) = \mathbf{S}^T(x, y)$ . The kernels  $\mathbf{T}^*(x, y)$  and  $\mathbf{T}(x, y)$  change sign when evaluated with respect to the normals directed to the opposite sides of the curve in 2-D or a surface in 3-D.

After a limit-to-the-boundary procedure applied to (1) and (3) for points on smooth boundary parts, the following BIEs, sometimes called  $u$ -BIE and  $t$ -BIE, respectively, are obtained [3, 4, 25, 26]:

$$\frac{1}{2} u_k(x) = \int_{\Gamma} U_{kl}(x, y)t_l(y) \, d\Gamma(y) - \oint_{\Gamma} T_{kl}(x, y)u_l(y) \, d\Gamma(y), \tag{4a}$$

$x \in \Gamma_S, \quad k, l = 1, \dots, d$

$$\frac{1}{2} t_k(x) = \oint_{\Gamma} T_{kl}^*(x, y)t_l(y) \, d\Gamma(y) - \int_{\Gamma} S_{kl}(x, y)u_l(y) \, d\Gamma(y), \tag{4b}$$

Considering a spherical (3-D) or circular (2-D) vanishing neighbourhood of the point  $x \in \Gamma_S$ , the second and first strongly singular integrals, respectively, on the right-hand sides of  $u$ -BIE and  $t$ -BIE are evaluated in the sense of Cauchy principal value, and the second hypersingular integral on the right-hand side of  $t$ -BIE is evaluated in the sense of Hadamard finite part [26].

Both aforementioned BIEs (4) are used in an SGBEM formulation. Only one of these equations is applied at points of a boundary part, depending on the boundary condition type defined on this boundary part. This approach leads to a symmetric integral operator of the first kind (according to the Fredholm theory of integral operators) in the formulation of the BIE system for SGBEM. Let us define partitions of the boundaries  $\Gamma_O$  and  $\Gamma_I$  depending on the type of boundary condition prescribed on each boundary part: for prescribed displacements  $\mathbf{u}$  and tractions  $\mathbf{t}$  subscripts ‘ $u$ ’ and ‘ $t$ ’ are used, respectively. Then,

$$\begin{aligned} \Gamma &= \bar{\Gamma}_u \cup \bar{\Gamma}_t, \quad \Gamma_u \cap \Gamma_t = \emptyset, \quad \mathbf{u}|_{\Gamma_u} = \tilde{\mathbf{u}}, \quad \mathbf{t}|_{\Gamma_t} = \tilde{\mathbf{t}} \\ \Gamma_I &= \bar{\Gamma}_{Iu} \cup \bar{\Gamma}_{It}, \quad \Gamma_{Iu} \cap \Gamma_{It} = \emptyset \\ \Gamma_O &= \bar{\Gamma}_{Ou} \cup \bar{\Gamma}_{Ot}, \quad \Gamma_{Ou} \cap \Gamma_{Ot} = \emptyset \end{aligned} \tag{5}$$

Either  $\Gamma_{Ou}$ ,  $\Gamma_{Ot}$ ,  $\Gamma_{Iu}$ ,  $\Gamma_{It}$  can be an empty set. In view of the objectives of the present work, the following analysis will be concerned with a particular case of a domain with traction boundary conditions prescribed on the cavity boundary, i.e.  $\Gamma_{It} = \Gamma_I$  and  $\Gamma_{Iu} = \emptyset$ . Then, the

following system of BIEs is obtained for SGBEM:

$$\begin{aligned}
 x \in \Gamma_{O_t} \cap \Gamma_S : & \int_{\Gamma_{O_t}} S_{kl}(x, y)u_l(y) \, d\Gamma(y) + \int_{\Gamma_{I_t}} S_{kl}(x, y)u_l(y) \, d\Gamma(y) - \int_{\Gamma_{O_u}} T_{kl}^{*+}(x, y)t_l(y) \, d\Gamma(y) \\
 & = \left( -\frac{1}{2} \tilde{t}_k(x) + \int_{\Gamma_{O_t}} T_{kl}^{*+}(x, y)\tilde{t}_l(y) \, d\Gamma(y) \right) + \int_{\Gamma_{I_t}} T_{kl}^{*+}(x, y)\tilde{t}_l(y) \, d\Gamma(y) - \int_{\Gamma_{O_u}} S_{kl}(x, y)\tilde{u}_l(y) \, d\Gamma(y)
 \end{aligned} \tag{6a}$$

$$\begin{aligned}
 x \in \Gamma_{I_t} \cap \Gamma_S : & \int_{\Gamma_{O_t}} S_{kl}(x, y)u_l(y) \, d\Gamma(y) + \int_{\Gamma_{I_t}} S_{kl}(x, y)u_l(y) \, d\Gamma(y) - \int_{\Gamma_{O_u}} T_{kl}^{*-}(x, y)t_l(y) \, d\Gamma(y) \\
 & = \int_{\Gamma_{O_t}} T_{kl}^{*-}(x, y)\tilde{t}_l(y) \, d\Gamma(y) + \left( -\frac{1}{2} \tilde{t}_k(x) + \int_{\Gamma_{I_t}} T_{kl}^{*-}(x, y)\tilde{t}_l(y) \, d\Gamma(y) \right) - \int_{\Gamma_{O_u}} S_{kl}(x, y)\tilde{u}_l(y) \, d\Gamma(y)
 \end{aligned} \tag{6b}$$

$$\begin{aligned}
 x \in \Gamma_{O_u} \cap \Gamma_S : & - \int_{\Gamma_{O_t}} T_{kl}^{+}(x, y)u_l(y) \, d\Gamma(y) - \int_{\Gamma_{I_t}} T_{kl}^{-}(x, y)u_l(y) \, d\Gamma(y) + \int_{\Gamma_{O_u}} U_{kl}(x, y)t_l(y) \, d\Gamma(y) \\
 & = - \int_{\Gamma_{O_t}} U_{kl}(x, y)\tilde{t}_l(y) \, d\Gamma(y) - \int_{\Gamma_{I_t}} U_{kl}(x, y)\tilde{t}_l(y) \, d\Gamma(y) + \left( \frac{1}{2} \tilde{u}_k(x) + \int_{\Gamma_{O_u}} T_{kl}^{+}(x, y)\tilde{u}_l(y) \, d\Gamma(y) \right)
 \end{aligned} \tag{6c}$$

where the plus and minus signs in the kernels  $T(x, y)$  and  $T^*(x, y)$  refer to the used normal vectors  $n^+$  and  $n^-$ , respectively.

Note that analysis developed in the present work can be easily generalized to cases where mixed boundary conditions are prescribed on a boundary part, which is not done here for the sake of simplicity of explanation.

### 2.2. Rigid-body motions and related properties of the integral operators

An interior BVP (defined for a bounded domain, with or without cavities) with prescribed tractions along the whole boundary, i.e.  $\Gamma_t = \Gamma$ , does not have a unique solution, inasmuch as an RBM, having zero stresses associated, can be added to any solution of the BVP in displacements.

Let us denote a basis of the linear space of RBMs by  $\mu_k^\alpha(x)$  for  $x \in \Omega \cup \Gamma$  and  $\alpha = 1, \dots, n_d$  with  $n_d = 3$  for  $d = 2$  or  $n_d = 6$  for  $d = 3$ . This basis in 2-D can be defined by the following vectors:

$$\mu^1(x) = \begin{Bmatrix} 1 \\ 0 \end{Bmatrix}, \quad \mu^2(x) = \begin{Bmatrix} 0 \\ 1 \end{Bmatrix}, \quad \mu^3(x) = \begin{Bmatrix} -x_2 \\ x_1 \end{Bmatrix} \tag{7}$$

Very important properties of RBMs  $\mu^\alpha(x)$  follow if they are substituted together with the pertinent zero tractions into (1), (4a), (3) and (4b). Then, for a particular case  $\Omega = \Omega^+$ ,

we obtain

$$\chi_{\Omega^+}(x)\mu_k^\alpha(x) + \int_{\Gamma_I} T_{kl}^+(x, y)\mu_l^\alpha(y) d\Gamma(y) = 0, \quad x \in \mathbb{R}^d \setminus \Gamma_I \tag{8a}$$

$$\frac{1}{2}\mu_k^\alpha(x) + \int_{\Gamma_I} T_{kl}^+(x, y)\mu_l^\alpha(y) d\Gamma(y) = 0, \quad x \in \Gamma_I \cap \Gamma_S \tag{8b}$$

$$\int_{\Gamma_I} S_{kl}(x, y)\mu_l^\alpha(y) d\Gamma(y) = 0, \quad x \in \mathbb{R}^d \setminus \Gamma_I \tag{9a}$$

$$\int_{\Gamma_I} S_{kl}(x, y)\mu_l^\alpha(y) d\Gamma(y) = 0, \quad x \in \Gamma_I \cap \Gamma_S \tag{9b}$$

Relations (8b) and (9b) express that the RBMs of the boundary  $\Gamma_I$  form the null space (space of eigenvectors associated to zero eigenvalue) of the integral operators on the left-hand side of these relations. In particular, relations (9) are of crucial importance for the present work.

Another important relation for RBMs can be obtained when RBMs are applied as solutions of the auxiliary problem in the second Betti theorem of reciprocity of works [4, 19, 23] written for a bounded body  $\Omega$ . It results in the following global equilibrium conditions for any solution in tractions of a BVP on  $\Omega$ :

$$\int_{\Gamma} t_k(x)\mu_k^\alpha(x) d\Gamma(x) = 0, \quad \alpha = 1, \dots, n_d \tag{10}$$

Naturally, RBMs are closely related to the situations where the system of BIEs used in SGBEM is not uniquely solvable.

As has been explained above, in the case of a bounded  $\Omega$  with  $\Gamma = \Gamma_t$ , any RBM of the whole domain  $\mu^\alpha$ , with associated zero stresses, causes non-uniqueness in the solution of the corresponding traction BVP, and consequently also a non-uniqueness in the solution of the BIE system used in SGBEM, which corresponds to the fact that the left-hand-side integrals in (6) vanish when evaluated for a  $\mu^\alpha$ . This issue has been studied in Reference [18] for domains without cavities.

Consider now a domain  $\Omega$ , bounded or unbounded, with a cavity. Let boundary displacements  $\mu_I^\alpha$  ( $\alpha = 1, \dots, n_d$ ) be defined as follows:

$$\mu_I^\alpha(x) = \begin{cases} \mu^\alpha(x) & \text{if } x \in \Gamma_I \\ \mathbf{0} & \text{if } x \in \Gamma_O \end{cases} \tag{11}$$

In simple terms,  $\mu_I^\alpha$  represent a RBM of the cavity boundary, keeping the outer boundary fixed.

As a consequence of (8a) and (9), it can be obtained that

$$\int_{\Gamma} T_{kl}^\pm(x, y)\mu_{Il}^\alpha(y) d\Gamma(y) = 0, \quad x \in \Gamma_O \tag{12a}$$

$$\int_{\Gamma} S_{kl}(x, y)\mu_{Il}^\alpha(y) d\Gamma(y) = 0, \quad x \in \Gamma \cap \Gamma_S \tag{12b}$$

Then, if traction boundary conditions are prescribed at the cavity  $\Omega^+$ , i.e.  $\Gamma_I = \Gamma_{It}$ , and the BIE system of SGBEM reduces to that in (6), a vector function  $\mathbf{f}$  defined on the boundary  $\Gamma$  as

$$\mathbf{f}(x) = \begin{cases} \boldsymbol{\mu}^\alpha(x) & \text{if } x \in \Gamma_I \\ \mathbf{0} & \text{if } x \in \Gamma_{Ou} \cup \Gamma_{Ot} \end{cases} \quad (13)$$

when substituted as the integral density into the integrals on the left-hand side of (6) causes them to vanish. Thus,  $\mathbf{f}$  represents a function which may be added to any solution of (6). The system is then non-uniquely solvable and its left-hand-side integral operator has the function  $\mathbf{f}$  in its null space.

Note that any  $\mathbf{f}$  defined above is in the null space of the operator on the left-hand side of (6) independently of the type of boundary conditions prescribed on  $\Gamma_O$ , in particular even if  $\Gamma_O = \Gamma_{Ou}$ .

The situation of more cavities can be treated in a similar way, functions  $\mathbf{f}$  now being associated to each cavity with boundary conditions prescribed only in tractions. In this manner each cavity of this type contributes by  $n_d$ -independent functions to the null space of the integral operator of the BIE system of SGBEM, see Appendix A.

It has to be stressed that this is not the case if the classical BEM based on  $u$ -BIE (4a) is applied at a cavity boundary with traction boundary conditions. In fact, if we choose (4a) instead of (4b) (Equation (6b)), we would obtain the following expression for the left-hand side of the equation associated to the cavity (at  $x \in \Gamma_{It} \cap \Gamma_S$ ):

$$\begin{aligned} & \int_{\Gamma_{Ot}} T_{kl}^+(x, y) f_l(y) d\Gamma(y) + \left( \frac{1}{2} f_k(x) + \int_{\Gamma_{It}} T_{kl}^-(x, y) f_l(y) d\Gamma(y) \right) \\ & + \int_{\Gamma_{Ou}} U_{kl}(x, y) f_l(y) d\Gamma(y) = 0 + \mu^\alpha(x) + 0 \neq 0 \end{aligned} \quad (14)$$

which means that the operator appearing in the BIE system of the classical BEM does not contain  $\mathbf{f}$  in its null space.

### 2.3. On the determination of the displacement solution of the BVP

Let us consider a one-cavity domain with  $\Gamma_I = \Gamma_{It}$ . Then, as follows from the analysis given in the previous section, any displacement solution of the BVP (which is unique if displacements are prescribed on some outer boundary part(s), i.e.  $\Gamma_{Ou} \neq \emptyset$ ) differs from the solution of the BIE system (6) by an RBM of the cavity boundary. Hence, even if we were able to find all the solutions of such a system, we might still be in trouble inasmuch as all we need in practice is that solution of the BIE system which is simultaneously the solution of the BVP. This solution can be found simply by a post-processing step that will be described below.

Let a displacement solution of (6) be denoted by  $\bar{\mathbf{u}}$  and the solution of BVP by  $\mathbf{u}$ . Then, the difference between these two functions is  $\bar{\mathbf{u}} - \mathbf{u} = \sum_{\alpha=1}^{n_d} \xi_\alpha \boldsymbol{\mu}_I^\alpha$  (see definition (11)),  $\xi_\alpha$  being



some constants. Let  $x \in \Omega$ . Then, we obtain from (1)

$$\begin{aligned} u_k(x) &= \int_{\Gamma} U_{kl}(x, y)t_l(y) \, d\Gamma(y) - \int_{\Gamma} T_{kl}(x, y)u_l(y) \, d\Gamma(y) \\ &= \int_{\Gamma} U_{kl}(x, y)t_l(y) \, d\Gamma(y) - \int_{\Gamma} T_{kl}(x, y)\bar{u}_l(y) \, d\Gamma(y) \end{aligned} \quad (15)$$

where the second equality holds due to (8a) in view of (11). We may now apply a limit process for  $\Omega \ni x \rightarrow x_0 \in \Gamma_I$ . Then, from the well known jump properties (e.g. References [3, 19, 23]), easily deduced from a comparison of (1) and a generalization of (4a) for any boundary point, including corner and edge points, we obtain

$$\begin{aligned} u_k(x_0) &= \int_{\Gamma} U_{kl}(x_0, y)t_l(y) \, d\Gamma(y) - \lim_{x \rightarrow x_0} \left( \int_{\Gamma} T_{kl}(x, y)\bar{u}_l(y) \, d\Gamma(y) \right) \\ &= \int_{\Gamma} U_{kl}(x_0, y)t_l(y) \, d\Gamma(y) - \int_{\Gamma} T_{kl}(x_0, y)\bar{u}_l(y) \, d\Gamma(y) + (\delta_{kl} - C_{kl}(x_0))\bar{u}_l(x_0) \end{aligned} \quad (16)$$

where  $C_{kl}(x_0)$  is the coefficient tensor of the free term in  $u$ -BIE, evaluated analytically for isotropic materials as shown in Reference [27].

Therefore, the evaluation of the correct displacement solution of BVP  $\mathbf{u}$  starting from a solution  $\bar{\mathbf{u}}$  of (6), when it is non-uniquely solvable, is reduced to an evaluation of the last member of (15) for a point in the interior of the domain and of (16) for the cavity boundary.

Note that the solution of (6) in displacements and tractions on the outer boundary coincides with the solution of the BVP.

### 3. NON-UNIQUENESS REMOVAL TECHNIQUES FOR SGBEM SYSTEMS

BVPs whose solutions are not unique frequently appear in modelling practical problems in engineering. Nevertheless, as was explained above, SGBEM with BIE system defined in (6) may have non-unique solution, even in some cases where the original BVP has a unique solution. If this is the case, then also the system of linear algebraic equations obtained after discretization of (6) may have more than one solution, i.e. its matrix is, at least theoretically, singular. Of course, numerically it may lead to a regular matrix, but very ill-conditioned, which can cause trouble in its solution. Thus, it seems to be very useful to introduce techniques which remove this non-uniqueness and replace the original BIE system (6) by a new one with only one solution.

#### 3.1. A method based on application of support conditions

A common way in engineering practice of treating with a BVP which allows some RBMs is to place some additional point supports which hinder these RBMs and do not introduce additional stresses in the body. This procedure corresponds in the numerical solution to a replacement of some rows and the corresponding columns of the matrix of the linear system by zeros

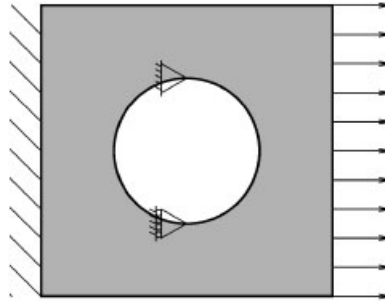


Figure 2. An application at the cavity boundary of point supports which do not introduce additional stresses in Method *S* in SGBEM.

everywhere (including the corresponding rows in the right-hand-side vector), except for the diagonal terms which are put equal, e.g. to unity. If the rows are properly chosen, the matrix becomes regular, and thus has only one solution. This is the most simple method, which will be referred to hereinafter as *Method S*, following the notation introduced in References [16, 18].

This method may be applied to SGBEM not only for BVPs whose boundary conditions allow an RBM of the whole body, but also, although it might not be clear at first sight, for BVPs on domains with a cavity whose boundary conditions do not avoid an RBM of the cavity boundary when considered independently of the rest of the body. It is possible to inhibit all these RBMs by applying point supports at the outer boundary (in the case of RBMs of the whole body) and at the cavity boundary. A simple example of an application of these supports is shown in Figure 2: at the top point of the cavity all displacements are constrained, at the bottom point only the horizontal one, which removes two rigid body translations and one rotation. In a numerical solution of the SGBEM system this method, as described in the previous paragraph, is as simple as replacing some rows and the corresponding columns by off-diagonal zeros and on-diagonal unities, a reasonably conditioned matrix being obtained in this way. Note that this method does not affect the symmetry of the system matrix.

It is clear that fixing by these point supports the solution of SGBEM obtained in this way is not the solution of the original BVP, the difference between these two solutions, as explained in Section 2.3, being given by some RBMs of the cavity boundary. The correct solution in displacements can be obtained in post-processing using (16).

### 3.2. Methods based on the Fredholm theory

The Fredholm theory provides an appropriate tool for integral operators which have a number of independent zero eigenfunctions equal to the number of independent functions orthogonal to the range of the operator [19, 20]. In our case the integral operator on the left-hand side of (6) is symmetric, the condition being naturally satisfied. Moreover, as implied from Section 2.2, the basis of the null space consists of allowed RBMs of the whole boundary,  $\mu^\alpha$ , and allowed RBMs of the boundary of the cavity subjected to traction,  $\mu_1^\alpha$ .

Let us denote the operator at the left-hand side of (6) by  $\mathcal{A}$ , the right-hand-side operator by  $\mathcal{B}$  and the vector functions which define unknown and prescribed boundary data by

$\mathbf{y}$  and  $\mathbf{b}$ , respectively, which means that

$$\mathbf{y}(x) = \begin{cases} \mathbf{u}(x), & x \in \Gamma_{I_t} \cup \Gamma_{O_t}, \\ \mathbf{t}(x), & x \in \Gamma_{O_u}, \end{cases} \quad \mathbf{b}(x) = \begin{cases} \tilde{\mathbf{t}}(x), & x \in \Gamma_{I_t} \cup \Gamma_{O_t} \\ \tilde{\mathbf{u}}(x), & x \in \Gamma_{O_u} \end{cases} \quad (17)$$

Thus, the original SGBEM system (6) reads as

$$(\mathcal{A}\mathbf{y})(x) = (\mathcal{B}\mathbf{b})(x), \quad x \in \Gamma \quad (18)$$

Let  $n_t$  denote the total number of linearly independent zero eigenvectors of the operator  $\mathcal{A}$ . Then,  $n_t = n_d$  if displacement boundary conditions are prescribed on some outer boundary part(s), i.e.  $\Gamma_{O_u} \neq \emptyset$ , or domain is unbounded, considering (2); otherwise  $n_t = 2n_d$ . We should note that if more than one cavity is present, each cavity with tractions prescribed contributes additionally by  $n_d$  linearly independent eigenvectors, see Appendix A.

According to References [16, 18], where other references can be found, two general methods can be applied to obtain an invertible operator on the left-hand side of a new system of equations whose solution also satisfies the SGBEM system (6).

The first one, denoted hereinafter, following References [16, 18], as *Method F1*, is based on augmenting the original SGBEM system, maintaining its symmetry, rendering:

$$(\mathcal{A}\mathbf{y}^{(1)})(x) + \sum_{\alpha=1}^{n_t} \mathbf{v}^\alpha(x) \omega^\alpha = (\mathcal{B}\mathbf{b})(x), \quad x \in \Gamma \quad (19a)$$

$$\int_{\Gamma} \mathbf{v}^\alpha(x) \mathbf{y}^{(1)}(x) \, d\Gamma(x) = 0, \quad \alpha = 1, \dots, n_t \quad (19b)$$

with an unknown vector  $\mathbf{y}^{(1)}$  and real constants  $\omega^\alpha$ .

The second method, denoted, again following References [16, 18], as *Method F2*, modifies the original operator  $\mathcal{A}$  by adding a symmetric operator with a degenerated kernel as follows:

$$(\mathcal{A}\mathbf{y}^{(2)})(x) + \sum_{\alpha=1}^{n_t} \mathbf{v}^\alpha(x) \int_{\Gamma} \mathbf{v}^\alpha(y) \mathbf{y}^{(2)}(y) \, d\Gamma(y) = (\mathcal{B}\mathbf{b})(x), \quad x \in \Gamma \quad (20)$$

It should be noted that both methods are directly related to problems searching for a stationary point of the functional  $\mathcal{F}$ :

$$\mathcal{F}(\mathbf{y}) = \frac{1}{2} \int_{\Gamma} \mathbf{y}(x) (\mathcal{A}\mathbf{y})(x) \, d\Gamma(x) - \int_{\Gamma} \mathbf{y}(x) (\mathcal{B}\mathbf{b})(x) \, d\Gamma(x) \quad (21a)$$

with restrictions

$$\int_{\Gamma} \mathbf{v}^\alpha(x) \mathbf{y}(x) \, d\Gamma(x) = 0, \quad \alpha = 1, \dots, n_t \quad (21b)$$

Method F1 corresponds to the solution of such a problem with Lagrange multipliers  $\omega^\alpha$ , whereas the elimination of the restriction conditions and including them into the integral equation system leads to Method F2.

Both these procedures can be applied only if the functions  $\mathbf{v}^\alpha(x)$  satisfy the relation:

$$\det \left[ \int_{\Gamma} \mathbf{v}^\alpha(x) \boldsymbol{\eta}^\beta(x) \, d\Gamma(x) \right]_{1 \leq \alpha, \beta \leq n_t} \neq 0 \tag{22}$$

where  $\boldsymbol{\eta}^\beta$  are defined by a basis of RBMs of the cavity boundary, e.g.  $\boldsymbol{\mu}_I^\alpha$  ( $\alpha = 1, \dots, n_d$ ), and, additionally, in the case of a bounded domain subjected exclusively to traction boundary conditions, they are given by a basis of the RBMs of the whole body, e.g.  $\boldsymbol{\mu}^\alpha$  ( $\alpha = 1, \dots, n_d$ ). This condition is a necessary and sufficient condition of invertibility of the operators on the left-hand side in (19) and (20), taking into account the symmetry of the operator  $\mathcal{A}$ . The proof of this statement for Method F1 and a general (symmetric or non-symmetric) operator was presented in References [19, 20]. After a slight modification it can be adopted for Method F2 as well. Condition (22) must thus be kept in mind when looking for a particular choice of functions  $\mathbf{v}^\alpha$ . The following basic relation between Methods F1 and F2 can be shown similarly as an analogous relation for the classical BIE in Reference [16]:

$$\int_{\Gamma} \mathbf{v}^\alpha(x) \mathbf{y}^{(2)}(x) \, d\Gamma(x) = \omega^\alpha = 0, \quad \alpha = 1, \dots, n_t \tag{23}$$

Consequently, both solutions,  $\mathbf{y}^{(1)}$  and  $\mathbf{y}^{(2)}$ , have to be equal because both satisfy the same constraint equations (19b) and (23).

In the following we will describe two natural choices of the functions  $\mathbf{v}^\alpha$  among an infinite number of possibilities.

The first approach, denoted as *Option M* (*M* referring to RBMs), is given by the most simple way of satisfying condition (22), defining  $\mathbf{v}^\alpha = \boldsymbol{\eta}^\alpha$ . It is obvious that (22) is then valid. Let us just recall that  $\boldsymbol{\eta}^\alpha$  form a basis (a set of linearly independent functions) of the null space of  $\mathcal{A}$  consisting of  $\boldsymbol{\mu}_I^\alpha$  and/or  $\boldsymbol{\mu}^\alpha$ . If this basis is orthonormalized (considering the usual inner product of the space  $L_2(\Gamma)$  of square-integrable functions over  $\Gamma$ ), defining a new basis of this null space,  $\tilde{\boldsymbol{\eta}}^\alpha$ , then the operator on the left-hand side of (20), i.e.

$$(\mathcal{A}\mathbf{y}^{(2)})(x) + \varepsilon \sum_{\alpha=1}^{n_t} \tilde{\boldsymbol{\eta}}^\alpha(x) \int_{\Gamma} \tilde{\boldsymbol{\eta}}^\alpha(y) \mathbf{y}^{(2)}(y) \, d\Gamma(y) = (\mathcal{B}\mathbf{b})(x), \quad x \in \Gamma \tag{24}$$

has the same eigenvalues as  $\mathcal{A}$ , except for the zero eigenvalues, which are changed to  $\varepsilon$ , see Reference [22] for details.

The second approach, denoted as *Option IE* (*IE* referring to BIE), is presented, for the sake of simplicity, for BVPs with the non-uniqueness in the SGBEM system due only to the cavity subjected to tractions. In this approach extra collocation BIEs (which correspond to (19b)) are evaluated at some points  $x^\alpha \in \Omega^+ \cup \Gamma_I$ ,  $\alpha = 1, \dots, n_d$ . Let us consider, first, only points  $x^\alpha$  in the domain  $\Omega^+$ . Then, the Somigliana displacement identity (1) evaluated at these points reads (note that  $x^\alpha$  are placed outside the domain  $\Omega$ , thus no free term is present):

$$\begin{aligned} & \int_{\Gamma_{O_t}} T_{kl}^+(x^\alpha, y) u_l(y) \, d\Gamma(y) + \int_{\Gamma_{I_t}} T_{kl}^-(x^\alpha, y) u_l(y) \, d\Gamma(y) - \int_{\Gamma_{O_u}} U_{kl}(x^\alpha, y) t_l(y) \, d\Gamma(y) \\ & = \int_{\Gamma_{O_t}} U_{kl}(x^\alpha, y) \tilde{t}_l(y) \, d\Gamma(y) + \int_{\Gamma_{I_t}} U_{kl}(x^\alpha, y) \tilde{t}_l(y) \, d\Gamma(y) - \int_{\Gamma_{O_u}} T_{kl}^+(x^\alpha, y) \tilde{u}_l(y) \, d\Gamma(y) \end{aligned} \tag{25}$$

where  $k$  represents a suitably selected component for each particular collocation point  $x^\alpha$  and should therefore have been written as  $k^\alpha$ , but the index was omitted for simplicity. The functions  $v^\alpha$  are defined by the left-hand side of (25) via the relation

$$[v^\alpha]_l(x) = \begin{cases} T_{kl}^+(x^\alpha, x), & x \in \Gamma_{Ot} \\ T_{kl}^-(x^\alpha, x), & x \in \Gamma_{It} \\ -U_{kl}(x^\alpha, x), & x \in \Gamma_{Ou} \end{cases} \quad (26)$$

Nevertheless, in contrast to the formulation given by (19), it is suitable to modify the right-hand side of the SGBEM system in order to satisfy not only the condition of invertibility of the operator on the left-hand side, but also to provide the solution of the modified SGBEM system as the solution of the original BVP as well. Actually, this objective can be achieved defining functions  $w^\alpha$  as follows from the right-hand side of (25):

$$[w^\alpha]_l(x) = \begin{cases} U_{kl}(x^\alpha, x), & x \in \Gamma_{It} \cup \Gamma_{Ot} \\ -T_{kl}^+(x^\alpha, x), & x \in \Gamma_{Ou} \end{cases} \quad (27)$$

Then, the constraint conditions (19b) in Method F1 take the modified form:

$$\int_\Gamma v^\alpha(x) y^{(1)}(x) d\Gamma(x) = \int_\Gamma w^\alpha(x) b(x) d\Gamma(x), \quad \alpha = 1, \dots, n_t \quad (28)$$

Thus, in fact, we have added to the SGBEM system equations (25). Method F2 is then given by the following equation with the modified right-hand side:

$$(\mathcal{A}y)(x) + \sum_{\alpha=1}^{n_t} v^\alpha(x) \int_\Gamma v^\alpha(y) y(y) d\Gamma(y) = (\mathcal{B}b)(x) + \sum_{\alpha=1}^{n_t} v^\alpha(x) \int_\Gamma w^\alpha(y) b(y) d\Gamma(y) \quad (29)$$

Although the presented modification of the SGBEM system might seem quite cumbersome, it is beneficial from the point of view of its numerical solution. We stated in Section 2.3 that it is generally necessary to calculate the solution of a BVP, with tractions prescribed on the cavity boundary, in a post-processing step defined by (16). But in Option IE this post-processing step is not necessary as its solution satisfies the Somigliana displacement identity inside the cavity  $\Omega^+$ , through (25), thus it must be a solution of the BVP.

Nevertheless, there is still an unresolved question about the last modification technique. Is condition (22) satisfied? After substituting (26) into (22) with the non-uniqueness due only to the cavity, i.e.  $\eta^\beta = \mu_I^\beta$ , we have

$$\begin{aligned} & \det \left[ \int_\Gamma v^\alpha(x) \eta^\beta(x) d\Gamma(x) \right]_{1 \leq \alpha, \beta \leq n_d} \stackrel{(11)}{=} \det \left[ \int_{\Gamma_I} v^\alpha(x) \mu_I^\beta(x) d\Gamma(x) \right]_{\alpha, \beta} \\ & \stackrel{(26)}{=} \det \left[ \int_{\Gamma_I} T_{kl}^-(x^\alpha, x) \mu_{Il}^\beta(x) d\Gamma(x) \right]_{\alpha, \beta} \stackrel{(8a)}{=} \det \left[ \chi_{\Omega^+}(x^\alpha) \mu_k^\beta(x^\alpha) \right]_{\alpha, \beta} \\ & = \det[\mu_k^\beta(x^\alpha)]_{\alpha, \beta} \stackrel{?}{\neq} 0 \end{aligned} \quad (30)$$

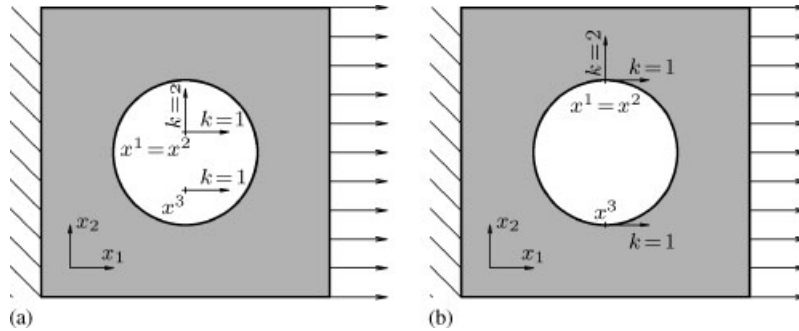


Figure 3. An application of additional Somigliana displacement identity collocations, which directly provides the solution of the BVP in Option IE in SGBEM: (a) collocations inside the cavity; and (b) collocations at the cavity boundary.

The numbers over the equation marks refer to the relations which prove the validity of the equations. The last term in (30) is not equal to zero, as long as Equation (25) is chosen in an adequate way, i.e. indices  $k$  and points  $x^\alpha$  represent collocations of the Somigliana displacement identity in directions  $k$  at points  $x^\alpha$  which do not allow the cavity boundary  $\Gamma_I$  to undergo an RBM. This configuration corresponds to point supports oriented in directions  $k$  and placed at positions  $x^\alpha$  in an elastic body defined by domain  $\Omega^+$  which would not allow any RBM of  $\Omega^+$ , see Reference [16] for a discussion of this condition. A simple example is shown in Figure 3(a).

What is the difference when points  $x^\alpha$  are chosen on the boundary  $\Gamma_I$ ? First of all, Equation (25) is considered being in the form of the  $u$ -BIE (4a). Considering only points  $x^\alpha$  placed at smooth parts of the boundary  $\Gamma_I$  we have

$$\int_{\Gamma_{Ot}} T_{kl}^+(x^\alpha, y) u_l(y) d\Gamma(y) + \left( \frac{1}{2} u_k(x^\alpha) + \int_{\Gamma_{It}} T_{kl}^-(x^\alpha, y) u_l(y) d\Gamma(y) \right) - \int_{\Gamma_{Ou}} U_{kl}(x^\alpha, y) t_l(y) d\Gamma(y) \\ = \int_{\Gamma_{Ot}} U_{kl}(x^\alpha, y) \tilde{t}_l(y) d\Gamma(y) + \int_{\Gamma_{It}} U_{kl}(x^\alpha, y) \tilde{t}_l(y) d\Gamma(y) - \int_{\Gamma_{Ou}} T_{kl}^+(x^\alpha, y) \tilde{u}_l(y) d\Gamma(y) \quad (31)$$

Therefore, the definition of functions  $v^\alpha$  in relation (26) should be changed to the following expression:

$$[v^\alpha]_l(x) = \begin{cases} T_{kl}^+(x^\alpha, x), & x \in \Gamma_{Ot} \\ \frac{1}{2} \delta_{kl} \delta(x - x^\alpha) + T_{kl}^-(x^\alpha, x), & x \in \Gamma_{It} \\ -U_{kl}(x^\alpha, x), & x \in \Gamma_{Ou} \end{cases} \quad (32)$$

where  $\delta(x - x^\alpha)$  is the Dirac delta function, while definition (27) of functions  $w^\alpha$  does not need any modification.

A small distinction also appears in the chain of equations of proof (30). In the determinant after the second equation mark, due to (32), a term in the form  $\frac{1}{2} \mu_{lk}^\beta(x^\alpha) +$

$\int_{\Gamma_l} T_{kl}^-(x^\alpha, x) \mu_{ll}^\beta(x) d\Gamma(x)$  appears. Using property (8b), instead of (8a), the same term  $\mu_k^\beta(x^\alpha)$  is produced in the last determinant of (30). The reasoning for the correct choice of directions  $k$  and points  $x^\alpha$  is then as above. An example of location of these points on the cavity boundary is shown in Figure 3(b).

Note that the point  $x^\alpha$  cannot be chosen outside the cavity, because due to Equation (8a) the value of the characteristic function  $\chi_{\Omega^+}(x^\alpha)$  would be zero, and consequently, also the determinant in (30) would vanish, causing condition (22) to fail.

Finally, let us just remark that Option IE is also applicable to remove the non-uniqueness in BVPs on bounded domains with the whole boundary subjected to tractions. The corresponding procedure, which removes RBMs  $\mu^\alpha$  from the null space of  $\mathcal{A}$ , consists in an application of either (1) or (4a), respectively, evaluated at suitable points,  $x^\alpha \in \Omega$  or  $x^\alpha \in \Gamma_S$ , and in suitable directions, the values of the free terms in these extra BIEs being imposed as zero. In simple terms, this procedure corresponds to an application of point supports at  $x^\alpha$  in the corresponding directions.

#### 4. DISCRETIZATIONS AND NON-UNIQUENESS REMOVAL TECHNIQUES

Consider a Galerkin approach used to discretize (6) in the framework of BEM, which leads to a system of linear equations, see also (18):

$$\mathbf{A} \mathbf{y}_d = \mathbf{B} \mathbf{b}_d \tag{33}$$

with a symmetric matrix  $\mathbf{A} \in \mathbb{R}^{N \times N}$ . If this matrix is singular, then it is possible to apply discretized versions of (19) or (20) to make (33) uniquely solvable. Application of *Method F1* leads to

$$\begin{bmatrix} \mathbf{A} & \mathbf{V} \\ \mathbf{V}^T & \mathbf{0} \end{bmatrix} \begin{Bmatrix} \mathbf{y}_d^{(1)} \\ \boldsymbol{\omega} \end{Bmatrix} = \begin{Bmatrix} \mathbf{B} \mathbf{b}_d \\ \mathbf{0} \end{Bmatrix} \tag{34}$$

where  $\boldsymbol{\omega}$  is a vector of  $n_t$  additional unknown constants, and *Method F2* leads to

$$[\mathbf{A} + \mathbf{V} \mathbf{V}^T] \{\mathbf{y}_d^{(2)}\} = \{\mathbf{B} \mathbf{b}_d\} \tag{35}$$

where the matrix  $\mathbf{V} \in \mathbb{R}^{N \times n_t}$  must satisfy the following condition, similar to (22)

$$\det[\mathbf{V}^T \mathbf{M}] \neq 0 \tag{36}$$

with matrix  $\mathbf{M} \in \mathbb{R}^{N \times n_t}$ , whose columns form a basis of the null space of the matrix  $\mathbf{A}$ . These columns are defined hereinafter by the eigenvectors  $\boldsymbol{\eta}^\beta$ ,  $\beta = 1, \dots, n_t$ . Notice that these RBMs can be exactly approximated by the boundary element functions when linear or higher-order boundary elements are considered.

The above discretized forms of Methods F1 and F2 can also be obtained by searching for a stationary point of a quadratic form with restrictions, similar to (21). Actually, the method of Lagrange multipliers applied to the quadratic form with restrictions:

$$\varphi(\mathbf{y}) = \frac{1}{2} \mathbf{y}^T \mathbf{A} \mathbf{y} - \mathbf{y}^T \mathbf{B} \mathbf{b}_d, \quad \mathbf{V}^T \mathbf{y} = \mathbf{0} \tag{37}$$

leads to (34) and the elimination of the restriction leads to (35).

Two choices of matrices  $\mathbf{V}$  corresponding to the two particular choices, called Options M and IE, of functions  $v^z$  discussed in Section 3.2 will be introduced below.

In *Option M*,  $\mathbf{V} = \mathbf{M}$ . Thus, the fulfilment of condition (36) is straightforward.

Let us see how to obtain a discretized version of (24). Consider a matrix  $\tilde{\mathbf{M}}$  with orthonormalized columns of  $\mathbf{M}$  [22]. Then, defining  $\mathbf{V}\mathbf{V}^T$  in (35) as  $\varepsilon\tilde{\mathbf{M}}\tilde{\mathbf{M}}^T$ , the modified matrix of the resulting system has the same spectrum as the original matrix  $\mathbf{A}$ , except for zero eigenvalues, which are replaced by  $\varepsilon$  [22].

In *Option IE*,  $\mathbf{V}$  is obtained through a discretization of the Somigliana displacement identity collocated at some adequately defined supports, see (25) and (31). These collocation equations, written in the following form analogous to (28), will replace the extra equations in Method F1 (34):

$$\mathbf{V}^T \mathbf{y}_d^{(1)} = \mathbf{W}^T \mathbf{b}_d \quad (38)$$

When Method F2 is used, the matrix on the right-hand side of (35) is modified in a similar way as in (29), obtaining

$$[\mathbf{A} + \mathbf{V}\mathbf{V}^T] \{\mathbf{y}_d^{(2)}\} = [\mathbf{B} + \mathbf{V}\mathbf{W}^T] \{\mathbf{b}_d\} \quad (39)$$

The proof of the continuous version of condition (36), presented in (30), can also be applied here to show that (36) is fulfilled by the matrix  $\mathbf{V}$  in Option IE.

It is an easy exercise to show, following the same reasoning as in Reference [16, see p. 4031 therein], that the difference  $\mathbf{y}_d^{(1)} - \mathbf{y}_d^{(2)}$  belongs to the null space of  $\mathbf{A}$ , and moreover that  $\mathbf{V}^T \mathbf{y}_d^{(2)} = \boldsymbol{\omega}$  in Option M and  $\mathbf{V}^T \mathbf{y}_d^{(2)} = \boldsymbol{\omega} + \mathbf{W}^T \mathbf{b}_d$  in Option IE. Therefore, if the original system (33) has a solution (which is what always happens except for the case of non-equilibrated discretized tractions prescribed over all the boundary in interior BVPs, see discussion in Reference [18]), then  $\boldsymbol{\omega} = \mathbf{0}$  and solutions  $\mathbf{y}_d^{(1)}$  and  $\mathbf{y}_d^{(2)}$  solve (33) and are equal to each other except for rounding-off errors.

Finally, let us mention that Method S can also be interpreted as a variant of Method F1, the matrix  $\mathbf{V}^T$  being defined by the point support equations [16].

## 5. NUMERICAL EXAMPLES

Two examples of plane BVPs have been solved using the methods of removal of the non-uniqueness in the SGBEM solution discussed in the previous sections. Traction boundary conditions are prescribed on the boundary of the cavities in both examples studied.

First, an exterior BVP given by a plane with a circular cavity subjected to far-field tension is presented.

Second, inasmuch as domains with more cavities can be treated similar to one-cavity domains, see Appendix A, the influence of the presence of cavities (one or two) on the solution accuracy is studied in an interior BVP.

A plane strain state is assumed in all instances. Material parameters Young's modulus and Poisson's ratio are  $E = 100$  GPa and  $\nu = 0.25$ , respectively. Dimensions of solids and displacements are given in millimeters.

The problems presented have been solved by a 2-D SGBEM code. The code uses linear continuous elements with nodes at the ends of the element allowing discontinuity of tractions



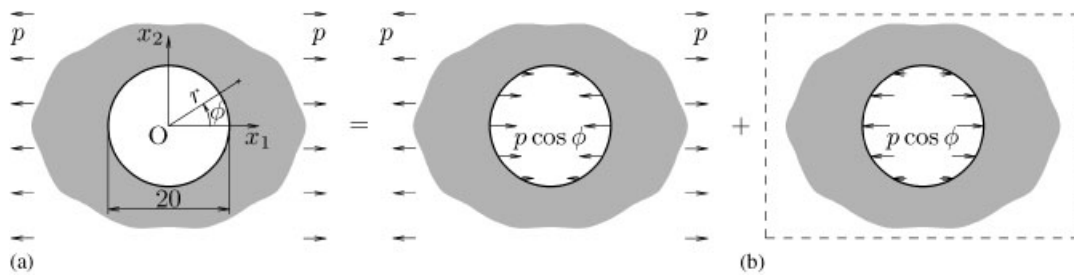


Figure 4. An infinite plate with a circular cavity: (a) problem configuration; and (b) removing of stresses and displacements at infinity by superposition.

when necessary. Thus, the curved contours of the boundaries are approximated by polygons. The integrals in the influence matrices are calculated analytically and Gauss elimination method is applied for solution of the discretized linear equation system. Double precision floating point arithmetic (REAL(8) in FORTRAN90) is used in all calculations.

The results of the following three methods of removal of the non-uniqueness in the solution of SGBEM are compared in the next sections:

S—Direct application of point support conditions, Section 3.1.

F2/M—In the continuous case this method is represented by (24), and its discrete form is given by (35) with  $\mathbf{V} = \sqrt{\varepsilon} \tilde{\mathbf{M}}$ ,  $\varepsilon = 0.5$ .

F2/IE—In the continuous case this method is represented by (29) together with (26), (27) and (32), and its discrete form is given by (39).

According to a discussion performed in Section 4, results of the corresponding variants of Method F1 are expected to coincide with those presented here for the two variants of Method F2 except for rounding-off errors. In the case of the interior BVP with a non-equilibrated discretized external load, these results may slightly differ by an element of the null space of the original linear system, see Reference [18].

### 5.1. Exterior Neumann problem: circular cavity in an infinite plate under uniaxial tension

A typical example of a uniquely solvable BVP, which, however, leads to a non-uniquely solvable BIE in SGBEM, is a problem of a single circular cavity in an infinite plate subjected to a uniaxial tension at infinity, Figure 4(a). Due to the fact that the analytical solution of this problem [28] does not fulfil condition (2), it is necessary to apply a superposition principle, Figure 4(b). Thus, numerical results have been calculated for the loading inside the cavity, see the framed configuration in Figure 4(b). The expression in polar co-ordinates for the Airy stress function in this case reads

$$F(r, \phi) = -\frac{p}{4} \left[ 2a^2 \ln r + \left( \frac{a^4}{r^2} - 2a^2 \right) \cos 2\phi \right], \quad p = 100 \text{ MPa}, \quad a = 10 \text{ mm} \quad (40)$$

In the numerical solution the cavity boundary is discretized using a uniform mesh of 80 straight elements.

Boundary displacements in radial and tangential directions,  $u_r$  and  $u_\phi$ , respectively, calculated applying Methods S, F2/M and F2/IE followed by the post-processing step described in

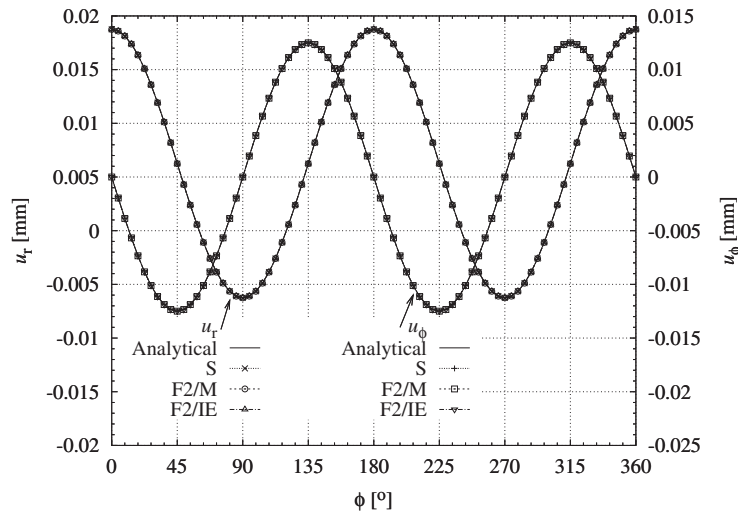


Figure 5. Results for the circular-cavity problem after application of post-processing by (16).

Section 2.3, are shown in Figure 5. An excellent agreement has been obtained between numerical and analytical solutions for all the methods applied. Note that the post-processing step is in fact not required for Method F2/IE (see (29) and the text below) and it has been applied here only for the purpose of an analysis of the effect of this step presented at the end of this section.

As expected, no influence of the application of point supports in Method S can be observed. These supports have been placed to satisfy the following conditions:

$$u_1(10, 0) = 0, \quad u_2(10, 0) = 0, \quad u_2(-10, 0) = 0 \quad (41)$$

The extra equations (25) used in Method F2/IE have been obtained by collocating  $u$ -BIE at points  $x^1(-5, 0)$ , with  $k=1$ ,  $x^2(-5, 0)$  with  $k=2$  and  $x^3(5, 0)$  with  $k=2$ . It is recommended that these points should not be placed very close to each other, in order to avoid a possible ill-conditioning of the resulting linear system. They have been chosen in the interior of the cavity but, as was explained in Section 3.2, they could also have been placed on the cavity boundary.

Normalized errors are depicted in Figure 6. There is no visible difference between the numerical results obtained by different methods for non-uniqueness removal. This is in agreement with the fact that all these numerical solutions are solutions of the original system (33), thus they differ only by an RBM of the cavity boundary, this difference being removed when (16) is applied. Note that this observed fact is independent of the degree of refinement of the mesh, the magnitude of errors changing with the mesh refinement but not the similarity between the results obtained by different methods.

An influence of the post-processing step, Section 2.3, upon the accuracy of results of Method F2/IE is shown in Figure 7, where normalized errors both before (F2/IE) and after (F2/IE+Post) application of this step are presented. Results obtained directly by Method F2/IE are more accurate than those obtained using (16) in this example. Thus, the most

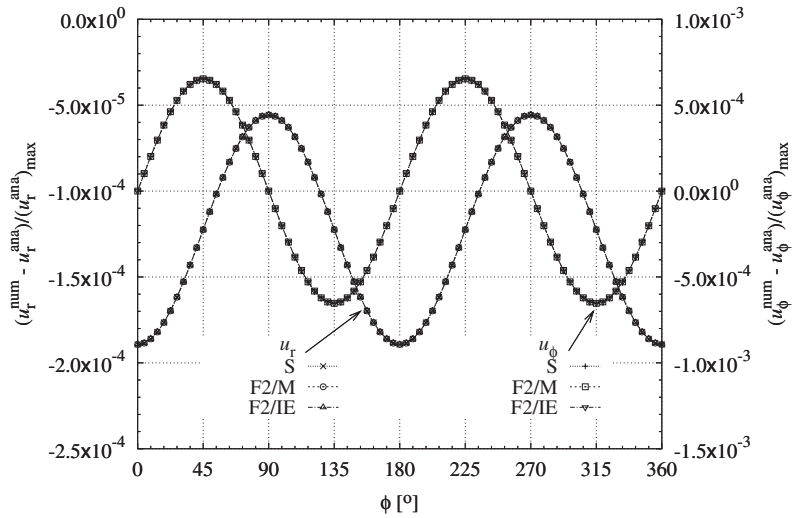


Figure 6. Normalized errors for the circular-cavity problem after the post-processing step.

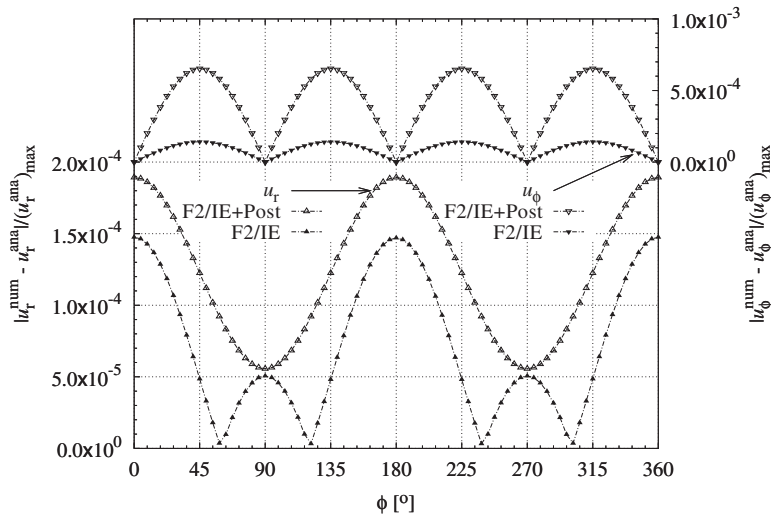


Figure 7. Absolute values of normalized errors obtained by Method F2/IE for the circular-cavity problem before and after the post-processing using boundary integral representation (16).

accurate results in this example correspond to a direct application of Method F2/IE with no post-processing. Nevertheless, this relation of errors cannot be considered to be general, as an inverse situation has also been observed in other examples.

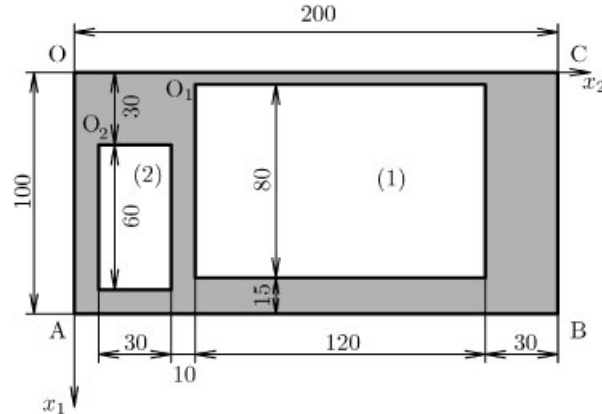


Figure 8. Geometry of a bounded domain with two cavities (1) and (2).

### 5.2. Bounded domains with cavities

Numerical solution of interior BVPs defined on a domain with cavities whose geometry is charted in Figure 8 will be analysed in this section. An analytical solution defined by the following Airy stress function has been considered here:

$$F(x_1, x_2) = F_0 \sin\left(\frac{x_1}{h}\right) \exp\left(-\frac{x_2}{h}\right), \quad F_0 = 10^4 \text{ N}, \quad h = 100 \text{ mm} \quad (42)$$

Two cases will be studied, first the domain with only one cavity, cavity (1) in Figure 8, and second the domain with both cavities. To obtain a uniquely solvable BVP with a non-invertible BIE operator, mixed boundary conditions will be applied here at the exterior boundary. Displacements are prescribed at faces  $OA$  and  $BC$ , and tractions at  $AB$  and  $CO$  and at cavity boundaries. A uniform mesh of boundary elements of length 10 mm has been used.

Let us start with the one-cavity case. The cavity has deliberately been placed extremely close to the exterior boundary in order to check the robustness and accuracy of the methods developed. Normalized errors in displacements at face  $AB$  are plotted in Figure 9,  $s$  being the arc length measured starting from point  $A$  in counterclockwise direction. It is possible to include also the results obtained directly by solving (33), without application of any method for non-uniqueness removal ('direct'), because the vectors in the null space of the matrix  $\mathbf{A}$  in (33) are zero for unknowns corresponding to the outer boundary. We can observe that quite accurate results, which coincide for all approaches, have been obtained.

The displacements at the cavity are depicted in Figure 10 with parameter  $s$  starting at point  $O_1$  in clockwise direction. Errors, which cannot be observed in this figure, are shown in Figure 11. The curves are plotted for all methods after the post-processing calculation (16). The additional constraints for Method S are applied at cavity (1) as follows:

$$u_1(5, 50) = 0, \quad u_2(5, 50) = 0, \quad u_1(5, 150) = 0 \quad (43)$$

The index 'a' in Method F2/IE refers to a particular choice of collocation equations (25) defined as follows:  $x^1(10, 60)$  with  $k=1$ ,  $x^2(10, 60)$  with  $k=2$  and  $x^3(80, 160)$  with  $k=1$ .

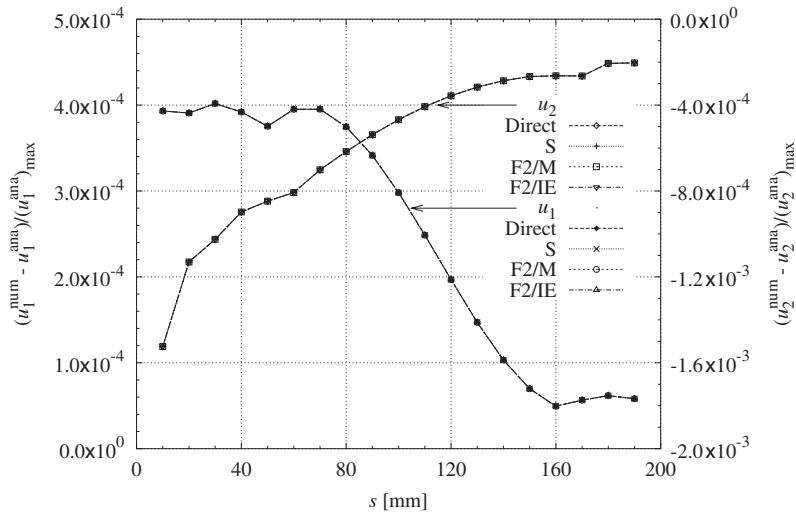


Figure 9. Normalized errors at face *AB* for the domain with one cavity.

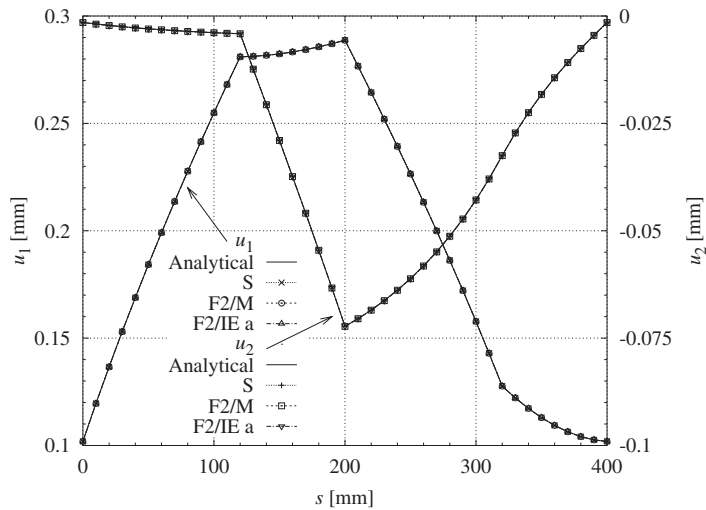


Figure 10. Results at cavity (1) for the domain with one cavity.

Results of all the methods coincide with each other (except for round-off errors), as could be expected in accordance with the related remark in Section 5.1.

Two aspects of the methods applied can be studied in Figure 12. First, we can observe the influence of points at which the Somigliana displacement identity (25) is collocated in Method F2/IE. It should be stressed that no post-processing has been used in this figure for Method F2/IE. Here, another choice with index ‘b’ has been introduced, its parameters being:  $x^1(35, 90)$  with  $k = 1$ ,  $x^2(35, 90)$  with  $k = 2$  and  $x^3(55, 130)$  with  $k = 1$ . The small gap

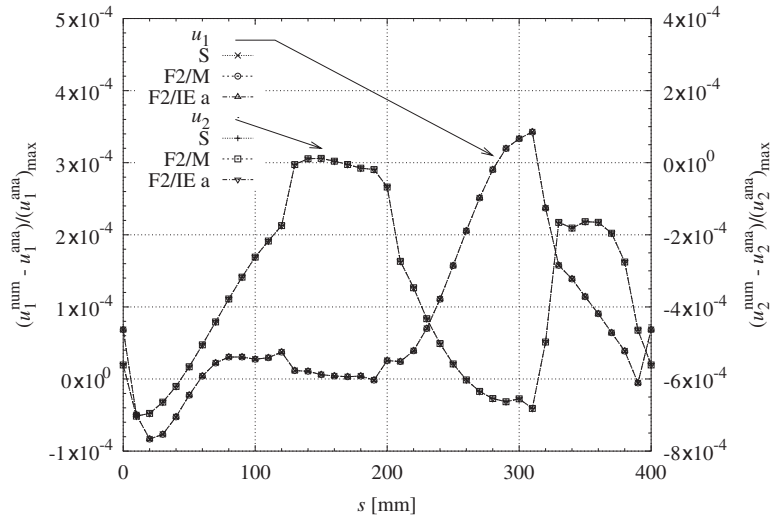


Figure 11. Normalized errors at cavity (1) for the domain with one cavity.

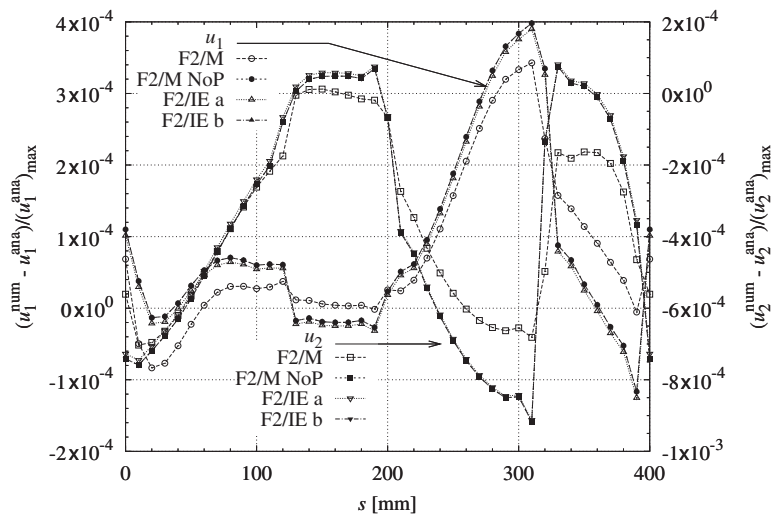


Figure 12. Normalized errors at cavity (1) for the domain with one cavity. Influence of post-processing and of positions of collocation points.

appearing between the two curves obtained by Method F2/IE is very interesting, because it is purely a very small RBM of the cavity boundary. Note that this could be expected, due to the fact that both solutions by Method F2/IE solve the original system (33).

Second, the effect of an application of the post-processing on the results by Method F2/M is studied. Results denoted as ‘F2/M NoP’ have been obtained from those by Method F2/M before the post-process calculation. They have been modified, subtracting an RBM, to obtain at

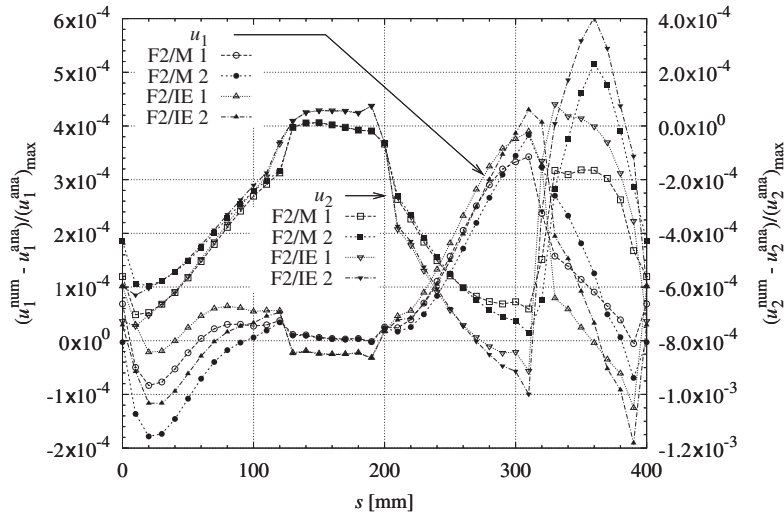


Figure 13. Normalized errors at cavity (1) for one-cavity and two-cavity cases.

some points the same value of the displacement as given by the ‘F2/IEb’ case, the following displacements being chosen in particular:  $u_1(5, 50)$ ,  $u_2(5, 50)$  and  $u_1(5, 60)$ . Then, the curves for these two procedures coincide everywhere. Thus, as a conclusion from the above results, it can be said that the only significant difference between results appears when the post-processing is applied. This is in agreement with the fact that solutions obtained by all the methods considered here before application of the post-processing solve (33). Let us also note that post-processing, unlike the example in Section 5.1, generates relatively smaller errors.

Let us now consider the case of the domain in Figure 8 with both cavities. Although the analysis in the theoretical part of the paper was performed only for one cavity, the results are applicable for multiple cavities as well, the only difference being that the number of linearly independent functions in the null space of the operator  $\mathcal{A}$  increases, see Section 2.2 and Appendix A. As in the case of cavity (1), the other cavity has been deliberately placed close to the outer boundary, and to cavity (1) too, in order to check the robustness and accuracy of the methods developed. As expected, the results, particularly at points of the cavity (1), are almost coincident with those obtained in the previous case considering only one cavity. The slight differences that appear between these two cases are due to the fact that we are solving two BVPs, equivalent in the sense that they have the same solution, but different in the sense that they have different domains leading to two distinct systems of linear equations. As in the previous case (only one cavity modelled) the results obtained with the three methods are almost coincident. For the sake of brevity, we show in Figure 13 only the displacements along the boundary of cavity (1). Normalized errors in displacements calculated using only two methods are presented in Figure 13 for the sake of clarity: ‘F2/M’ with post-processing and ‘F2/IE’ without it (collocation points  $x^\alpha$  and directions  $k$  in (25) being set as in option ‘a’ for cavity (1), see above, and as  $x^4(40, 20)$  with  $k = 1$ ,  $x^5(40, 20)$  with  $k = 2$  and  $x^6(80, 30)$  with  $k = 1$  for cavity (2)). The indices ‘1’ and ‘2’ at method marks in Figure 13 refer to the number of cavities taken into account in the domain.

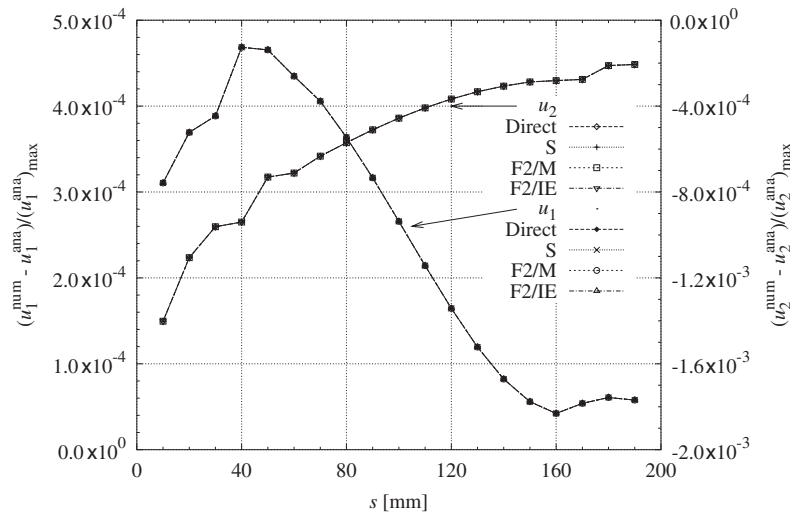


Figure 14. Normalized errors at face  $AB$  for the domain with two cavities.

Some differences between the results obtained for the two cases appear especially along the parts of the cavity boundary which are close to the other cavity in case '2' and at the face which is quite close to the outer boundary, but no additional differences appear in spite of the presence of the second cavity. Also comparing normalized errors in displacements at face  $AB$  of the outer boundary between the case of one cavity, Figure 9, and the case of two cavities, Figure 14, the only distinction is observed at the part of  $AB$  which is near to cavity (2).

## 6. CONCLUDING REMARKS

Two general methods for non-uniqueness removal in SGBEM, called Methods F1 and F2, have been presented and studied in the framework of the Fredholm theory of linear operators. Three particular variants of these methods, denoted as S, F2/M and F2/IE, have been implemented in an SGBEM code and the numerical results obtained by these methods for some BVPs have been analysed. A special case of a domain with only one cavity has been analysed in detail, although domains with multiple cavities can be treated as well, see Appendix A.

With reference to BVPs which are defined on either a bounded domain with displacements prescribed on some boundary part or an infinite domain, and which have a cavity subjected to tractions, the following observation has to be made: the methods developed in the present work lead to the same solution except for RBMs of the cavity boundary when considering all the methods before an application of post-processing step (16), and lead to the same solution except for round-off errors when all the methods after this step are considered. As has been explained, this is caused especially by the property of system (6) that always (in this kind of BVPs) has a solution, inasmuch as the range of the right-hand-side operator is the same as the range of the operator at the left-hand side, even in the case where the system is not uniquely solvable.



Thus, any solution of either the modified system (19) or (20) is the solution of the original system.

The objective of the following final comparative evaluation of the methods proposed in the present work is to provide a concise guide for selection of the most suitable method in accordance with the requirements and possibilities of each particular SGBEM code programmer.

Method S is the simplest one, and easily applicable. An analogous procedure is also successfully used in FEM codes. Nevertheless, it can produce non-acceptable results in the case of prescribed non-equilibrated discretized loads due to peaks appearing at point supports. Additionally, as can be seen in Appendix B, it seems to be the least stable method, because the condition number of the resulting linear system matrix depends relatively strongly on the position of the supports. Finally, it requires an application of post-processing step (16) to obtain the solution of the BVP.

Method F2/M is also very simple to implement, due to a simple representation of the RBMs within any discretization. It works satisfactorily for any solved problem. When comparing the condition number of the resulting linear system (see Appendix B), this method looks the best. Nevertheless, it needs an application of post-processing step (16) to obtain the solution of the BVP at cavities subjected to tractions.

In contrast to the two previous methods, Method F2/IE does not need post-processing step (16). This aspect may be useful in some applications, e.g. modelling contact problems of a bolt in a hole in 2-D. It has to be said, however, that its implementation is slightly more involved. The results obtained may also depend on the choice of the collocation points where the extra  $u$ -BIEs are evaluated. These points can be chosen in the interior or at the boundary of those cavities whose boundary conditions are prescribed in tractions exclusively. Collocation points inside the cavities have only been considered in the numerical examples presented, inasmuch as the influence of their position, inside or at the boundary of the cavity, on the accuracy of the results was not substantial.

As a general conclusion we can state that the removal of the non-uniqueness in SGBEM should be done in the framework of Methods F1 and F2. Options M and IE are the most recommended, each having some advantages in comparison with the other one. Therefore, the final decision will always depend on the particular conditions of each SGBEM code.

Another case of uniquely solvable BVPs whose SGBEM solutions are not unique, not dealt with in the present work, given by the 2-D BVPs with prescribed displacement boundary conditions for one or two critical sizes of the domain, has been studied in Reference [29]. Similar methods to those based on the Fredholm theory developed here can be applied to this case as well.

Finally, let us point out that the methods presented here can easily be adapted for applications of SGBEM to other elastic BVPs not considered in the present work (e.g. BVPs with mixed boundary conditions and contact problems) and also to other applications (e.g. potential theory).

#### APPENDIX A: NOTE ON THE DOMAINS WITH MORE CAVITIES

Consider a (bounded or unbounded) domain  $\Omega$  with more than one cavity. To analyse the non-uniqueness of the SGBEM solution in such a domain a slightly modified notation will be useful. The boundary  $\Gamma$  of such a domain is split into several components—the outer

boundary (if it exists) and boundaries of cavities. Let  $\Gamma_I$  denote the boundary of the  $I$ th cavity  $\Omega_I^+$  ( $I = 1, \dots, N_c$ ),  $N_c$  being the number of cavities. Let boundary displacements  $\mu_I^\alpha$  ( $\alpha = 1, \dots, n_d$ ) be defined, similar to (11), as follows:

$$\mu_I^\alpha(x) = \begin{cases} \mu^\alpha(x) & \text{if } x \in \Gamma_I \\ \mathbf{0} & \text{if } x \in \Gamma \setminus \Gamma_I \end{cases} \quad (\text{A1})$$

A similar reasoning to that used in deduction of (12) leads to

$$\int_{\Gamma} T_{kl}^{\pm}(x, y) \mu_{II}^\alpha(y) d\Gamma(y) = 0, \quad x \in \Gamma_J, \quad J \neq I \quad (\text{A2a})$$

$$\oint_{\Gamma} S_{kl}(x, y) \mu_{II}^\alpha(y) d\Gamma(y) = 0, \quad x \in \Gamma \cap \Gamma_S \quad (\text{A2b})$$

Let the cavities be numbered in such a way that the first  $N_{ct}$  of them have only traction boundary conditions prescribed, i.e.  $\Gamma_J = \Gamma_{Jt}$ , for  $J = 1, \dots, N_{ct}$ . Consider a BIE system for a multi-cavity domain similar to system (6) for one-cavity domain,  $\Gamma_I$  terms therein being split into  $\Gamma_J$  terms ( $J = 1, \dots, N_{ct}$ ) here. Then, boundary functions  $f_J$

$$f_J(x) = \begin{cases} \mu^\alpha(x) & \text{if } x \in \Gamma_J \\ \mathbf{0} & \text{if } x \in \Gamma \setminus \Gamma_J \end{cases} \quad (\text{A3})$$

substituted as the integral densities into the left-hand-side integrals of the pertinent BIE system cause them to vanish. Thus, the BIE system is non-uniquely solvable and its left-hand-side integral operator has functions  $f_J$  in its null space. Each cavity with prescribed traction contributes by  $n_d$ -independent functions to the null space of this integral operator. For example, a two-cavity domain in Section 5.2 leads to a linear operator which originally (i.e. before application of any method for the non-uniqueness removal proposed in the present work) has a six-dimensional null space.

Another question arises concerning the applicability of the methods discussed in Section 3. It should be stressed that all these methods can be used also for the domains with multiple cavities, though some remarks should be made. First, with reference to Method S, the support points are chosen for each cavity with prescribed tractions in the same way as for the one-cavity case. The methods based on the Fredholm theory were discussed considering two particular options, M and IE. Option M is directly applicable as the necessary and sufficient condition of applicability, (22), is naturally satisfied. Option IE deserves a brief analysis. First, Equations (25)–(27) (adapted for more cavities) should be introduced for each of the cavities  $\Omega_J^+$  with traction boundary conditions. The point  $x^\alpha$  can now be distinguished also by an index  $J$  referring to the number of the pertinent cavity, i.e. we denote it as  $x_J^\alpha$ . For simplicity of notation it is assumed that the non-uniqueness is only due to the cavities subjected to tractions. Then, the modification of the proof of the validity of condition (22),

presented in (30) for one cavity, can be sketched as follows:

$$\begin{aligned}
 & \det \left[ \int_{\Gamma} \mathbf{v}^{\hat{\alpha}}(x) \boldsymbol{\eta}^{\hat{\beta}}(x) \, d\Gamma(x) \right]_{1 \leq \hat{\alpha}, \hat{\beta} \leq n_t} \stackrel{(A1)}{=} \det \left[ \int_{\Gamma_I} \mathbf{v}_J^{\alpha}(x) \boldsymbol{\mu}_I^{\beta}(x) \, d\Gamma(x) \right]_{\substack{1 \leq \alpha, \beta \leq n_d \\ 1 \leq I, J \leq N_{c_t}}} \\
 & \stackrel{(26)}{=} \det \left[ \int_{\Gamma_I} T_{kl}^-(x_J^{\alpha}, x) \boldsymbol{\mu}_{II}^{\beta}(x) \, d\Gamma(x) \right]_{\alpha, \beta; I, J} \stackrel{(8a)}{=} \det \left[ \chi_{\Omega_I^+}(x_J^{\alpha}) \boldsymbol{\mu}_k^{\beta}(x_J^{\alpha}) \right]_{\alpha, \beta; I, J} \\
 & = \prod_{J=1}^{N_{c_t}} \det \left[ \boldsymbol{\mu}_k^{\beta}(x_J^{\alpha}) \right]_{\alpha, \beta} \stackrel{?}{\neq} 0 \tag{A4}
 \end{aligned}$$

The number  $n_t$ , as in Section 3.2, denotes the total number of linearly independent zero eigenvectors of the operator  $\mathcal{A}$  from (18) and it is equal to  $N_{c_t} n_d$ . The numbers over the equation marks refer to the relations which prove the validity of the equation. The last term, similar to that of (30) does not vanish, as long as additional equations according to (25) are chosen correctly, i.e. indices  $k$  and points  $x_J^{\alpha}$  represent collocations of the Somigliana displacement identity in directions  $k$  at points  $x_J^{\alpha}$  which do not allow the cavity boundary  $\Gamma_I$  to undergo an RBM.

### APPENDIX B: CONDITION NUMBERS FOR DIFFERENT METHODS

The objective of this appendix is to present a few numerical results that will characterize the influence of the methods for non-uniqueness removal in SGBEM presented in this work on the spectral properties and condition number of the resulting linear system.

In Table BI, the rows contain maximum  $\sigma_{\max}$  and minimum  $\sigma_{\min}$  singular values, obtained from the singular value decomposition (SVD) of the resulting linear system matrix, see Reference [30]. These maximum and minimum singular values are, in the case of a symmetric matrix, maximum and minimum eigenvalues taken in absolute value, the condition number  $\kappa$  being defined as a ratio between  $\sigma_{\max}$  and  $\sigma_{\min}$ .

With reference to results of all three methods for the exterior problem, Method F2/M, which (in the variant implemented in the present work) does not change the spectrum of the matrix, except for the zero eigenvalues, produces the smallest  $\kappa$ , while the other two methods cause

Table BI. Condition numbers and other parameters.

	Exterior problem			Interior problem						
	S1	F2/M	F2/IE	One Cavity				Two cavities		
				S1	F2/M	F2/IE 1	F2/IE 2	S1	F2/M	F2/IE
$\sigma_{\max}$	0.75587	0.7559	0.75587	1.3654	1.3686	1.3837	1.3686	1.3654	1.3686	1.3846
$\sigma_{\min}/10^{-4}$	51.331	523.06	60.599	2.9518	3.3959	3.4050	3.4050	2.9502	3.3979	3.3979
$\kappa$	147.25	14.451	124.73	4625.8	4030.3	4063.7	4019.5	4628.4	4028.1	4074.8

the smallest positive singular value in the modified linear system to be smaller than it was in the original SGBEM system.

When considering the results for the problem on the bounded domain with cavities, the most influential factor seems to be the presence of both BIEs,  $u$ -BIE and  $t$ -BIE, in the SGBEM system for a BVP with mixed type of boundary conditions. The different methods do not change the singular values significantly, leading to almost equal condition numbers.

Note that although the above-discussed spectral properties, and in particular the obtained values of the condition number, do not greatly affect the solution by Gauss elimination, they might be important for an iterative solver.

#### ACKNOWLEDGEMENTS

The authors acknowledge the financial support from the Scientific Grant Agency of the Slovak Republic (Grant No. 1/8033/01 and 1/1089/04) given to R.V. and from the Spanish Ministry of Education and Culture (Project No. MAT2003-03315) given to V.M. and F.P.

#### REFERENCES

1. Bonnet M, Maier G, Polizzotto C. Symmetric Galerkin boundary element method. *Applied Mechanics Review* 1998; **15**:669–704.
2. Sirtori S. General stress analysis by means of integral equations and boundary elements. *Meccanica* 1979; **14**:210–218.
3. Baláš J, Sládek J, Sládek V. *Stress Analysis by Boundary Element Method*. Elsevier: Amsterdam, 1989.
4. París F, Cañas J. *Boundary Element Method, Fundamentals and Applications*. Oxford University Press: Oxford, 1997.
5. Blázquez A, Vodička R, París F, Mantič V. Comparing the conventional displacement BIE and the BIE formulations of the first and the second kind in frictionless contact problems. *Engineering Analysis with Boundary Elements* 2002; **26**:815–826.
6. Vodička R, Mantič V. A comparative study of three systems of boundary integral equations in the potential theory. In *IUTAM/IACM/IABEM Symposium on Advanced Mathematical and Computational Mechanics Aspects of the Boundary Element Method*, Cracow, 1999, Burczynski T (ed.). Kluwer Academic Publishers: Dordrecht, 2001; 377–394.
7. Hackl K, Zastrow U. On the existence, uniqueness and completeness of displacements and stress functions in linear elasticity. *Journal of Elasticity* 1988; **19**:3–23.
8. Hsiao GC, Wendland WL. On a boundary integral method for some exterior problems in elasticity. *Proceedings of Tbilisi University, UDK 539.3, Math. Mech. Astron.*, 1985; 31–60.
9. Pérez-Gavilán JJ, Aliabadi MH. Symmetric Galerkin BEM for multi-connected bodies. *Communications in Numerical Methods in Engineering* 2001; **17**:761–770.
10. Pérez-Gavilán JJ, Aliabadi MH. A symmetric Galerkin BEM for multi-connected bodies: a new approach. *Engineering Analysis with Boundary Elements* 2001; **25**:633–638.
11. Power H, Miranda G. Second kind integral equation formulation of Stokes' flows past a particle of arbitrary shape. *SIAM Journal on Applied Mathematics* 1987; **47**(4):689–698.
12. Karrila SJ, Kim S. Integral equations of the second kind for Stokes flow: direct solution for physical variables and removal of inherent accuracy limitations. *Chemical Engineering Communications* 1989; **82**:123–161.
13. Kim S, Karrila SJ. *Microhydrodynamics: Principles and Selected Applications*. Butterworth-Heinemann: Boston, MA, 1991.
14. Phan-Thien N, Kim S. *Microstructures in Elastic Media: Principles and Computational Methods*. Oxford University Press: New York, 1994.
15. Phan-Thien N, Tullock D. Completed double layer boundary element method in elasticity. *Journal of the Mechanics and Physics of Solids* 1993; **41**(6):1067–1086.
16. Blázquez A, Mantič V, París F, Cañas J. On the removal of rigid body motions in the solution of elastostatic problems by direct BEM. *International Journal for Numerical Methods in Engineering* 1996; **39**:4021–4038.

17. Lutz E, Ye W, Mukherjee S. Elimination of rigid body modes from discretized boundary integral equations. *International Journal of Solids and Structures* 1998; **35**:4427–4436.
18. Vodička R, Mantič V, París F. Notes on the removal of rigid body motions in the solution of elastostatic problems by SGBEM. *Engineering Analysis with Boundary Elements*, in press.
19. Chen G, Zhou J. *Boundary Element Methods*. Academic Press: London, 1992.
20. Chen G, Sun S. Augmenting a Fredholm operator of zero index to achieve invertibility for elliptic boundary value problems. *Journal of Mathematical Analysis and Applications* 1993; **176**:24–48.
21. Greenbaum A, Greengard L, McFadden GB. Laplace's equation and the Dirichlet–Neumann map in multiply connected domains. *Journal of Computational Physics* 1993; **105**:267–278.
22. Heise U. Removal of the zero eigenvalues of integral operators in elastostatic boundary value problems. *Acta Mechanica* 1981; **41**:41–61.
23. Jaswon MA, Symm GT. *Integral Equation Methods in Potential Theory and Elastostatics*. Academic Press: London, 1977.
24. Mantič V, París F. Symmetry properties of the kernels of the hypersingular integral and the corresponding regularized integral in the 2D Somigliana stress identity for isotropic materials. *Engineering Analysis with Boundary Elements* 1997; **20**:63–168.
25. Guiggiani M, Krishnasamy G, Rudolphi TJ, Rizzo FJ. A general algorithm for the numerical solution of hypersingular boundary integral equations. *Journal of Applied Mechanics—Transactions of the ASME* 1992; **59**:604–614.
26. Mantič V, París F. Existence and evaluation of the free terms in the hypersingular boundary integral equation of potential theory. *Engineering Analysis with Boundary Elements* 1995; **16**:253–260.
27. Mantič V. A new formula for the C-matrix in the Somigliana identity. *Journal of Elasticity* 1993; **33**:191–201.
28. Timoshenko SP, Goodier JN. *Theory of Elasticity*. McGraw-Hill: New York, 1970.
29. Vodička R, Mantič V. On invertibility of elastic single layer potential operator. *Journal of Elasticity* 2004; **74**:147–173.
30. Golub GH, van Loan CF. *Matrix Computations*. The Johns Hopkins University Press: Baltimore, MD, 1983.